

# Dependence of microstructure of Al-44 at% and Al-48 at% zn alloys on temperature

---

Skoko, Željko; Popović, Stanko

Source / Izvornik: **Fizika A**, 2001, 10, 191 - 202

Journal article, Published version

Rad u časopisu, Objavljena verzija rada (izdavačev PDF)

Permanent link / Trajna poveznica: <https://um.nsk.hr/um:nbn:hr:217:642259>

Rights / Prava: [In copyright](#)/[Zaštićeno autorskim pravom.](#)

Download date / Datum preuzimanja: **2024-12-18**



Repository / Repozitorij:

[Repository of the Faculty of Science - University of Zagreb](#)



DEPENDENCE OF MICROSTRUCTURE OF Al-44 at% Zn AND Al-48 at% Zn  
ALLOYS ON TEMPERATURE

ŽELJKO SKOKO and STANKO POPOVIĆ

*Physics Department, Faculty of Science, University of Zagreb, Bijenička cesta 32,  
HR-10002 Zagreb, POBox 331, Croatia, E-mail address: SPOPOVIC@phy.hr*

**Dedicated to Professor Kseno Ilakovac on the occasion of his 70<sup>th</sup> birthday**

Received 15 November 2001; Accepted 14 January 2002  
Online 6 April 2002

The temperature dependence of microstructure of the title alloys was studied in situ by XRD. Each alloy had been subjected to two different thermal treatments: (i) rapid quenching from the solid-solution temperature,  $T_{SS}$ , in water at room temperature (RT) and ageing at RT (samples WQ) and (ii) cooling slowly from  $T_{SS}$  to RT and ageing at RT (samples SC). As the samples SC were closer to the equilibrium state than the samples WQ, the microstructure of the two sets of samples depended on temperature in a different way. The solid solution,  $\alpha_{SS}$ , was formed at about 720 K for the samples SC, and at about 880 K for the samples WQ. During the slow cooling to RT the samples SC and WQ behaved in a similar way. Instead of the phase transitions expected according to the phase diagram, the following sequence of transitions was observed for both alloys:  $\alpha(M/\beta)+\beta(Zn) - \alpha'+\beta(Zn)+\alpha(M/\alpha',\beta) - \alpha_{SS}$ . A similar thermal behaviour was also found for the Zn-rich alloys, Al-54 at% Zn and Al-62 at% Zn.

PACS numbers: 61.50.-f, 64.70, 64.75.-p, 64.75.+g, 65.70.+y

UDC 548.73

Keywords: Al-Zn alloys, solid solution, phase transition, phase diagram, X-ray powder diffraction

## 1. Introduction

The system Al-Zn has been studied by many authors with respect to its mechanical, thermal, electrical and chemical properties and microstructure. Most of the knowledge was collected in a recent comprehensive monograph (H. Löffler, editor) [1], containing several hundred references. Zinc atoms do not form intermetallic phases with Al atoms due to the weak mutual interaction. The difference in atomic

radius of the two elements (0.143 nm for Al, 0.134 nm for Zn) has an important influence on the microstructure of Al-Zn alloys.

The equilibrium state of an Al-Zn alloy can be reached after a prolonged ageing, say at room temperature (RT, 298 K). In this state, the alloy contains two phases, namely, the fcc  $\alpha$ -phase (the matrix, M), having about 99 at% Al, and the hexagonal  $\beta$ (Zn)-phase (the precipitates), having about 99.5 at% Zn. This means that the mutual solid solubility of Zn and Al at RT is small. The solubility of Zn in Al increases with temperature and reaches about 67 at% at about 655 K [1]. The alloy, rapidly quenched from the solid-solution temperature,  $T_{SS}$ , to RT, is supersaturated and undergoes a decomposition, during ageing at RT or at elevated temperature, in the following general way: spherical Guinier-Preston zones (GPZ, fcc, fully coherent with M, having the radius of 1 to 2 nm and containing about 70 at% Zn) – ellipsoidal GPZ (fcc, fully coherent with M) – rhombohedrally distorted  $\alpha'_R$ -phase (partially coherent with M, with particles having about 10 nm in size) – metastable  $\alpha'$ -phase (fcc, partially coherent with M) –  $\beta$ (Zn)-phase (incoherent with M, particle size of the order of 1  $\mu\text{m}$ ) [1]. During ageing at RT a direct transition of big GPZ to  $\beta$ (Zn) is possible [2, 3]. The decomposition rate is dependent on the quenched-in vacancies, the initial Zn content and the ageing temperature [1–5]. The equilibrium phase diagram of the system has been defined on the basis of a number of papers and accepted in the literature [1, 6].

Nevertheless, a need appeared recently to perform a more detailed and accurate study of the microstructure of Al-Zn alloys, by X-ray powder diffraction (XRD), in dependence on the initial alloy compositions, previous thermal treatment and temperature [2–5, 7–11]. The alloys of different composition, ranging from 3 to 62 at% Zn, were quenched rapidly from  $T_{SS}$  to RT and aged at RT or at elevated temperature. These alloys were supersaturated solid solutions, which decomposed, and the precipitation processes were followed in detail [2, 3, 8]. Also, the alloys of different initial content of Zn, having reached the equilibrium state, were subjected to a gradual change of temperature, from RT to  $T_{SS}$ , and back to RT, and their microstructure was followed in situ by XRD [7, 9–11]. These studies have resulted in much new information, e.g., on the zinc content in the matrix and in different types of precipitates, P, in contact with M, on the strains occurring at the M/P interfaces, on the unit-cell parameter of M,  $a[\alpha(\text{M/P})]$ , on the unit-cell parameters of the metastable phase  $\alpha'$ ,  $a(\alpha')$ , of the equilibrium phase  $\beta$ (Zn),  $a(\beta)$  and  $c(\beta)$ , and of the solid solution  $\alpha_{SS}$ ,  $a(\alpha_{SS})$ . The recent studies have shown that a change in the phase diagram is necessary in the region where the initial contents of Al and Zn are similar.

In a previous paper, a detailed study of the temperature dependence of the microstructure of two Al-Zn alloys in the Zn-rich region was described, namely Al-54 at% Zn and Al-62 at% Zn [11]. The present paper describes similar experiments performed on two Al-Zn alloys in the Al-rich region, namely Al-44 at% Zn and Al-48 at% Zn. The aim of these two studies has been to compare the temperature behaviour of the two groups of alloys, taken in the Al-rich and in the Zn-rich region, and to study consequences of the obtained results on the phase diagram of the Al-Zn system.

## 2. Experimental

The powder samples for XRD were prepared by filing the bulk alloys, produced from elements of purity 4 N. The samples were annealed for 2 hours in a vertical furnace, in the region of the solid solution temperature. One set of samples (one of each alloy) was rapidly quenched inside the furnace from 770 K in water at RT, and then aged at RT for 7 (the alloy with 48 at% Zn) or 14 (the alloy with 44 at% Zn) days. The estimated quenching rate was  $10^5$  K/s. These samples were denoted as "water quenched" samples, WQ. A detailed quenching procedure was described in the previous papers [9,11]. The other set of samples (one of each alloy) was slowly cooled over 5 days from 720 K to RT and then aged at RT for 7 (the alloy with 48 at% Zn) or 14 (the alloy with 44 at% Zn) days ("slowly cooled samples", SC). Both sets of samples, being quenched/slowly cooled and aged at RT tended to the equilibrium state. One may suppose that, after ageing, the SC samples were much closer to the equilibrium state than the WQ samples. Different ageing times of the samples at RT were chosen because the decomposition processes were faster in the alloy with a higher Zn content. After ageing at RT, the samples were studied by XRD using a Philips diffractometer having a high-temperature attachment, a proportional counter and a graphite monochromator, with  $\text{CuK}\alpha$  radiation. The samples were heated (by a Pt strip) from RT to  $T_{\text{SS}}$  and then cooled back to RT, at a rate of about 2 K/min. The heating/cooling of the samples was stopped at a series of temperatures (20 to 30) for 15 to 20 minutes in order to scan prominent diffraction line profiles. The sample Al-48 at% Zn, WQ, was subjected to two heating and cooling cycles, between RT and  $T_{\text{SS}}$ . The samples were exposed to air ( $10^5$  Pa), but in accordance with previous studies the results did not depend on air pressure (between  $10^{-3}$  and  $10^5$  Pa) [7, 9–11]. The diffraction patterns taken at RT before heating and after a complete heating and cooling cycle were very similar; this was a proof that experiments were performed in a perfect way.

All precautions were undertaken in order to minimize systematic aberrations which could influence the derived values of the unit-cell parameters of the phases  $\alpha$ ,  $\alpha'$ ,  $\alpha_{\text{SS}}$  and  $\beta(\text{Zn})$  [12, 13].

## 3. Results and discussion

According to the phase diagram [1, 6], one could expect the following phase transitions for the alloys Al-44 at% Zn and Al-48 at% Zn:  $\alpha(\text{M}/\beta)+\beta(\text{Zn}) - \alpha'+\alpha(\text{M}/\alpha') - \alpha_{\text{SS}}$ . Instead, the following sequence of phase transitions has been observed for both alloys,

$$\alpha(\text{M}/\beta)+\beta(\text{Zn}) - \alpha' +\beta(\text{Zn})+\alpha(\text{M}/\alpha',\beta) - \alpha_{\text{SS}}.$$

This result, as well as the one from Ref. [11], indicates that a correction in the phase diagram of the system Al-Zn is necessary.

Prominent diffraction lines, at medium Bragg angles, of the alloy Al-48 at% Zn at selected temperatures (scanned in situ at a given temperature), including

two complete heating and cooling cycles, are shown in Fig. 1. These diffraction line profiles belong to the WQ sample. The dependence of the unit-cell parameter,  $a$ , of the phases  $\alpha$ ,  $\alpha'$  and  $\alpha_{SS}$  in the alloy Al-48 at% Zn, on temperature during the first heating from RT to  $T_{SS}$ , and cooling back to RT is shown in Fig. 2 for the WQ sample, and in Fig. 3 for the SC sample. The arrows indicate the

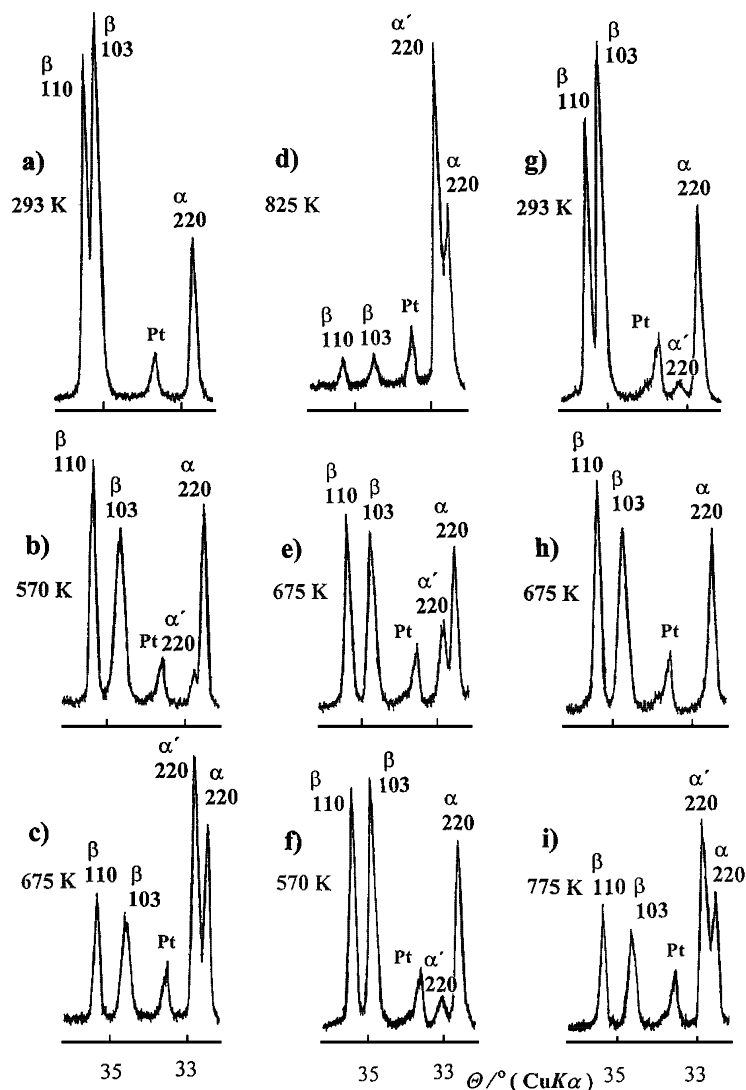


Fig. 1. Prominent diffraction lines of the alloy Al-48 at% Zn at selected temperatures, including both the first and second heating and cooling cycle. The alloy was quenched from the solid-solution temperature,  $T_{SS}$ , to RT (in water) and aged at RT for 7 days. Radiation: monochromatized (graphite)  $\text{CuK}\alpha$ , counter: proportional.

sense of the temperature change, while vertical bars show the estimated standard deviation in the derived parameter values. The temperature dependence of the

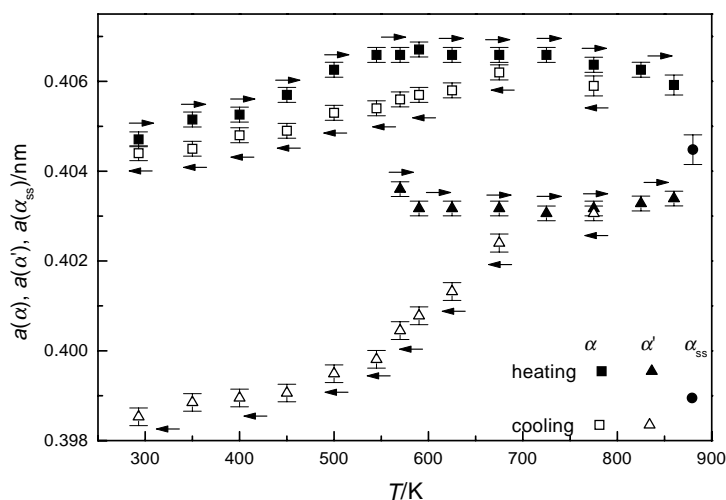


Fig. 2. Dependence of the unit-cell parameter,  $a$ , of the phases  $\alpha$ ,  $\alpha'$  and  $\alpha_{SS}$  in the water-quenched (WQ) alloy Al-48 at% Zn on temperature during the first heating from RT to  $T_{SS}$  and cooling to RT. The arrows indicate the sense of temperature change. Vertical bars indicate the estimated standard deviation (e.s.d.) in  $a$ .

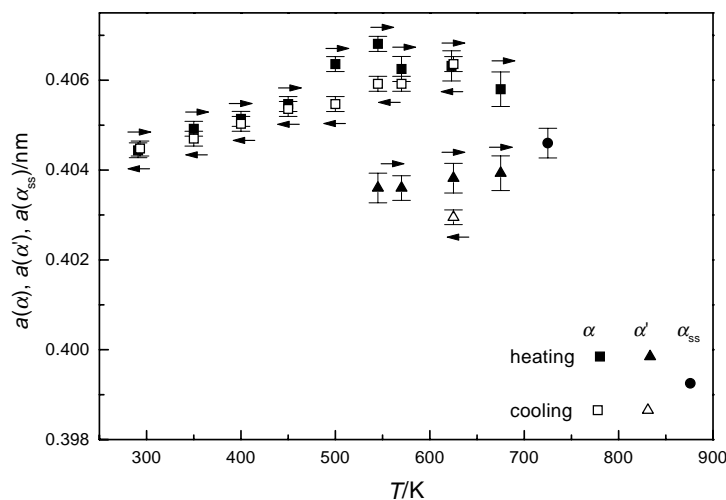


Fig. 3. Dependence of the unit-cell parameter,  $a$ , of the phases  $\alpha$ ,  $\alpha'$  and  $\alpha_{SS}$  in the alloy Al-48 at% Zn on temperature during the first heating from RT to  $T_{SS}$  and cooling to RT. The alloy was slowly cooled from  $T_{SS}$  to RT over 5 days and aged at RT for 7 days. The arrows indicate the sense of temperature change. Vertical bars indicate e.s.d. in  $a$ .

unit-cell parameters  $a(\beta)$  and  $c(\beta)$  of the  $\beta(\text{Zn})$  phase in the alloy Al-48 at% Zn during the first heating from RT to  $T_{\text{SS}}$  and cooling back to RT is shown in Figs.

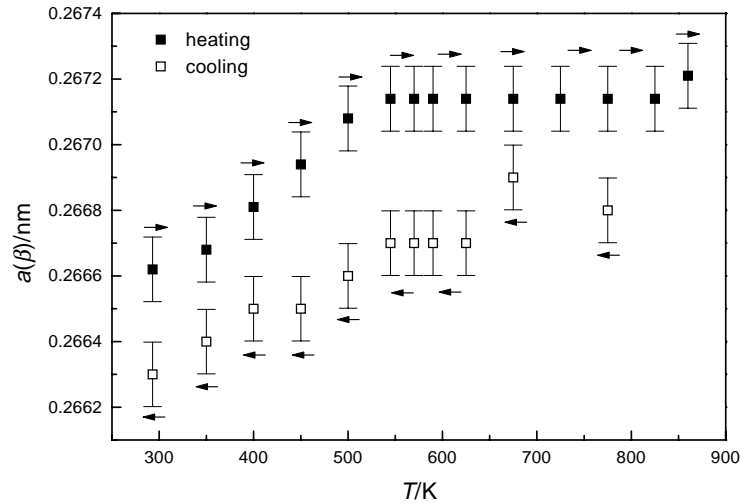


Fig. 4. Dependence of the unit-cell parameter  $a(\beta)$  of the phase  $\beta(\text{Zn})$  in the water quenched (WQ) alloy Al-48 at% Zn on temperature during the first heating from RT to  $T_{\text{SS}}$  and cooling to RT. The arrows indicate the sense of temperature change. Vertical bars indicate e.s.d. in  $a(\beta)$ .

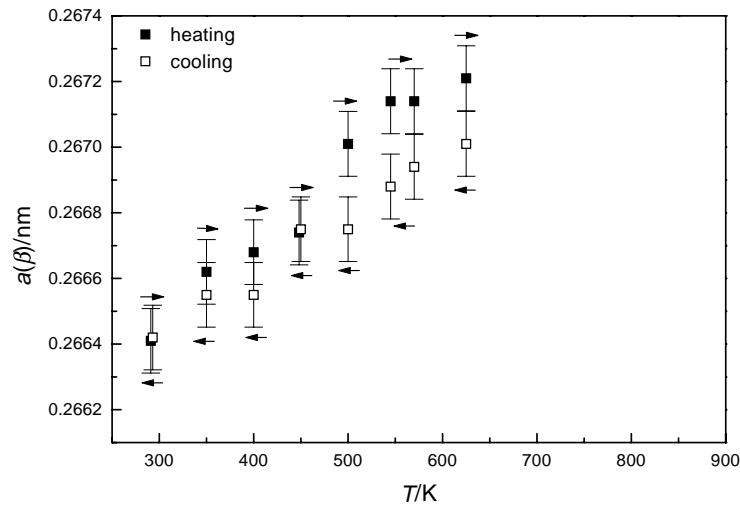


Fig. 5. Dependence of the unit-cell parameter  $a(\beta)$  of the phase  $\beta(\text{Zn})$  in the slowly-cooled (SC) alloy Al-48 at% Zn on temperature during the first heating from RT to  $T_{\text{SS}}$  and cooling to RT. The arrows indicate the sense of temperature change. Vertical bars indicate e.s.d. in  $a(\beta)$ .

4 and 6, respectively, for the WQ sample, and in Figs. 5 and 7, respectively, for the SC sample. Similar temperature behaviour was also observed for the alloy

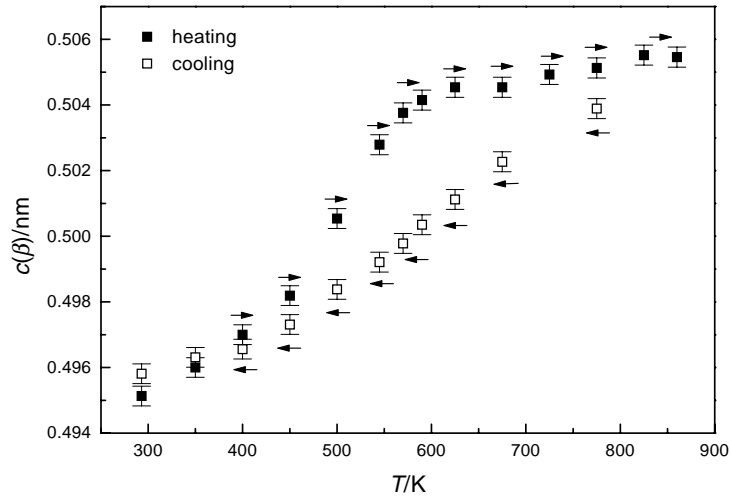


Fig. 6. Dependence of the unit-cell parameter  $c(\beta)$  of the phase  $\beta(\text{Zn})$  in the water-quenched (WQ) alloy Al-48 at% Zn on temperature during the first heating from RT to  $T_{\text{SS}}$  and cooling to RT. The arrows indicate the sense of temperature change. Vertical bars indicate e.s.d. in  $c(\beta)$ .

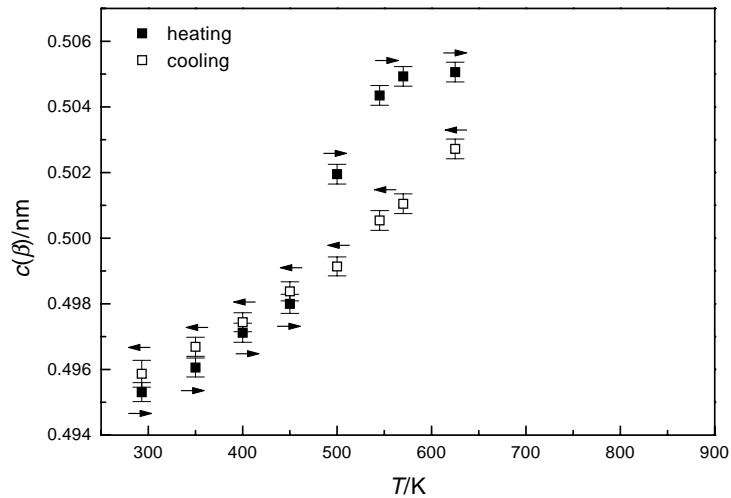


Fig. 7. Dependence of the unit-cell parameter  $c(\beta)$  of the phase  $\beta(\text{Zn})$  in the slowly cooled (SC) alloy Al-48 at% Zn on temperature during the first heating from RT to  $T_{\text{SS}}$  and cooling to RT. The arrows indicate the sense of temperature change. Vertical bars indicate e.s.d. in  $c(\beta)$ .



Al-44 at% Zn. The volume fraction of particular phases changed with temperature, and this manifested in the change of the diffraction line intensities. As an example, the temperature dependence of the peak intensity of the diffraction lines 110 and 103 of the phase  $\beta(\text{Zn})$  for the alloy Al-44 at% Zn during the first heating and cooling cycle is shown in Fig. 8 for the SC sample.

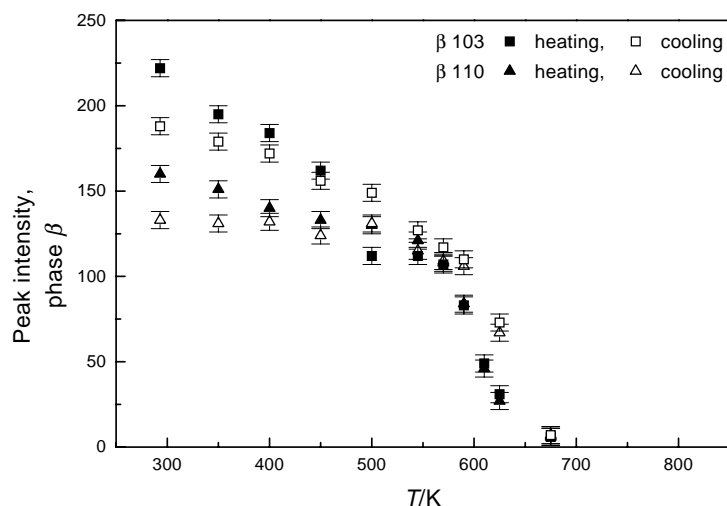


Fig. 8. Dependence of peak intensity of diffraction lines 110 and 103 of the phase  $\beta(\text{Zn})$  on temperature for the alloy Al-44 at% Zn during the first heating and cooling cycle. The alloy was slowly cooled from  $T_{\text{SS}}$  to RT over 5 days and aged at RT for 14 days. Vertical bars indicate e.s.d. in peak intensity.

By comparison of Figs. 2, 4 and 6 with Figs. 3, 5 and 7, one can conclude that the temperature dependence of the microstructure of the WQ sample is different from that of the SC sample. The two curves, which would show this dependence during the first heating from RT to  $T_{\text{SS}}$  and cooling from  $T_{\text{SS}}$  to RT, are closer to each other for the SC sample than for the WQ sample. The curves corresponding to the second heating from RT to  $T_{\text{SS}}$  and cooling from  $T_{\text{SS}}$  back to RT are closer to the ones for the first cooling from  $T_{\text{SS}}$  to RT than to the ones for the first heating from RT to  $T_{\text{SS}}$ , for the WQ sample.

The unit-cell parameter of the  $\alpha(\text{M}/\beta)$ -phase, in equilibrium with the  $\beta(\text{Zn})$ -phase, reached after a prolonged ageing of the quenched alloy, does not depend on the initial alloy composition, amounting 0.40469(6) nm at RT. However, the unit-cell parameter of the  $\alpha(\text{M}/\beta)$ -phase for the alloys, which reach the equilibrium state by slow cooling from  $T_{\text{SS}}$  to RT and ageing at RT, is 0.40445(10) nm at RT, regardless of the initial alloy composition [2, 3, 9]. The difference between these two equilibrium values of  $a[\alpha(\text{M}/\beta)]$  is due to different contents of Zn retained in the matrix, as a result of different thermal treatments. Previous and present studies show that the unit-cell parameters of the  $\beta(\text{Zn})$ -phase, in equilibrium with the  $\alpha(\text{M}/\beta)$ -phase, are close to those of pure Zn at RT,  $a = 0.2665(2)$ ,  $c = 0.4947(3)$

nm (space group  $P6_3/mmc$ ).

Let us describe, firstly, general features of the temperature dependence of microstructure of the WQ samples. As the temperature of the alloy increases, a decrease of the diffraction line intensities of both  $\alpha(M/\beta)$ - and  $\beta(\text{Zn})$ -phases takes place, due to the enhanced thermal vibrations of the atoms. A gradual shift of the diffraction lines toward smaller Bragg angles is observed, caused by thermal expansion (Figs. 1, 2, 4 and 6). Thermal expansion of the  $\beta(\text{Zn})$ -phase is anisotropic. It can be followed, for instance, from the temperature dependence of the angular separation of adjacent diffraction lines 110 and 103 of the  $\beta(\text{Zn})$ -phase (Fig. 1). Thermal expansion along the  $c$ -axis is several times bigger than along the  $a$ -axis of the  $\beta(\text{Zn})$ -phase, in accordance with the result in Ref. [11]. An indication of the thermal expansion anisotropy may also be a decrease of the saddle intensity between the diffraction line profiles 110 and 103, as the temperature increases (Fig. 1). Besides, one can also observe a change of the shape of the  $\beta(\text{Zn})$  precipitates with the increase of temperature. This follows from the broadening (Fig. 1) of the diffraction lines with  $l \neq 0$  (e.g. 002, 103) in relation to the diffraction lines with  $l = 0$  (e.g. 100, 110). The precipitates of the  $\beta(\text{Zn})$ -phase become more and more flat, i.e. their size along the  $c$ -axis decreases as the temperature increases. Zinc atoms, which leave the  $\beta(\text{Zn})$  precipitates, are dominantly those that form the lattice planes (001). One may suppose that the concentration of vacancies in the  $\beta(\text{Zn})$ -phase increases with temperature, and this affects the temperature dependence of its  $a$  and  $c$  unit-cell parameters (Figs. 4 and 6).

During the first heating, the unit-cell parameter,  $a$ , of the  $\alpha(M/\beta)$ -phase changes approximately linearly up to about 500 K (Fig. 2). At a higher temperature, a partial dissolution of Zn-atoms from the  $\beta(\text{Zn})$ -phase in the  $\alpha(M/\beta)$ -phase takes place. As the Zn atoms are smaller than the Al atoms, this dissolution of Zn atoms compensates and even reverses the change of the unit-cell parameter  $a$  of the  $\alpha(M/\beta)$ -phase with temperature (Fig. 2). A new phase,  $\alpha'$  (fcc), appears above about 550 K, in accordance to the phase diagram [1, 6]. Its diffraction lines are at the higher-angle side of diffraction lines of the  $\alpha$ -phase. According to the phase diagram, the  $\alpha$ -phase should be in coexistence with the  $\alpha'$ -phase above 550 K, i.e. the  $\beta(\text{Zn})$ -phase should completely transform into  $\alpha'$  phase above that temperature. However, the present results, as well as the results from the previous work [11], show that only a partial transition of the  $\beta(\text{Zn})$ -phase, and probably a partial transition of the  $\alpha(M/\beta)$ -phase, into the fcc  $\alpha'$ -phase takes place above 550 K. Therefore, the  $\alpha$ -phase is in coexistence with both  $\alpha'$ - and  $\beta(\text{Zn})$ -phases above 550 K, and is denoted as  $\alpha(M/\alpha',\beta)$ . The unit-cell parameter  $a$  of the  $\alpha'$ -phase is about 0.85% smaller than the one of the  $\alpha(M/\alpha',\beta)$ -phase at 590 K, due to different contents of zinc in the two phases. On further heating, the peak intensity of diffraction lines of the  $\alpha'$ -phase increases, while the one of the diffraction lines of the  $\beta(\text{Zn})$ -phase decreases. The composition of the phases changes, the content of Zn in the  $\alpha(M/\alpha',\beta)$ -phase increases, while in the  $\alpha'$ -phase decreases. The content of Al in the  $\beta(\text{Zn})$ -phase probably increases (Figs. 4 and 6). At about 880 K a solid solution  $\alpha_{\text{SS}}$  (fcc), is formed. The unit-cell parameter of the solid solution at 880 K is 0.4045(1) and 0.4046(1) nm for the alloys with 48 and 44 at% Zn, respectively

(Fig. 2).

During cooling from  $T_{SS}$  to RT, the dependence of the microstructural parameters on temperature is closer to a linear one, than during the heating from RT to  $T_{SS}$ . The intensity of diffraction lines of the  $\alpha'$ -phase decreases during cooling more rapidly, than it increased during the heating, i.e. at a given temperature, the intensity is smaller in the cooling run than in the heating run. The opposite is observed for the  $\beta(\text{Zn})$  phase (Figs. 1c and e). A small fraction of the  $\alpha'$ -phase is observed even at RT (Fig. 1g). In the repeated, second, heating of the same specimen of the Al-48 at% Zn alloy, a temperature delay in phase transitions of several tens of K takes place in relation to the first heating (Figs. 1c, e and h). During the second cooling, the microstructural parameters exhibit a similar dependence on temperature as during the second heating, and similar to that during the first cooling.

The general features, observed in the temperature dependence of microstructure of WQ samples, are also observed with the SC samples. At a given temperature, the difference between the values of a microstructural parameter, found in the heating run and in the cooling run, is smaller for the SC samples than for the WQ samples (this follows from a comparison of Figs. 2 and 3, 4 and 5, 6 and 7). Figure 8 shows the change of the peak intensity of the diffraction lines 110 and 103 of the  $\beta(\text{Zn})$ -phase with temperature for the alloy Al-44 at% Zn. In the case of SC samples, the solid solution,  $\alpha_{SS}$ , is formed at about 720 K.

#### 4. Conclusion

The temperature dependence of the microstructure of the alloys Al-44 at% Zn and Al-48 at% Zn is strongly influenced by the previous thermal treatments of the alloys. One set of samples was rapidly quenched from the solid-solution temperature,  $T_{SS}$ , in water at RT (samples WQ), and the other set of samples was slowly cooled from  $T_{SS}$  to RT (samples SC). Both sets of samples were aged at RT for a short period. The different behaviour of the two sets of samples in relation to the change of temperature follows from the fact that they had different starting microstructure before examination by XRD. The SC samples were much closer to the equilibrium state than were the WQ samples. One may suppose for the WQ samples that the precipitates  $\beta(\text{Zn})$  were not uniformly distributed in the  $\alpha(\text{M}/\beta)$ -phase, and residual strains in the  $\alpha(\text{M}/\beta)$ -phase around the  $\beta(\text{Zn})$  precipitates were present. A very important fact is that the number of quenched-in vacancies at RT was much bigger in the WQ samples than in the SC samples. The first heating of the WQ samples was slow, at a rate of about 2 K/min, and the samples were held for 15 to 20 minutes at a number of temperatures in order to record diffraction patterns. The first cooling was performed in a similar way. Therefore, it may be supposed that most of strains in the WQ samples were annealed during the first heating and cooling. This resulted in a microstructure at RT, which was different from the starting microstructure at RT, concerning the size and shape of the  $\beta(\text{Zn})$  precipitates, their distribution in the  $\alpha(\text{M}/\beta)$ -phase, and strains around the  $\beta(\text{Zn})$

precipitates. The number of vacancies might be also smaller than in the starting WQ samples. The vacancies play a dominant influence on the diffusion rate of Zn atoms, explaining the delay in phase transitions during the second heating in relation to the first heating.

In Ref. [11] only the WQ samples of the alloys Al-54 at% Zn and Al-62 at% Zn, i.e., the alloys in the Zn-rich region, were studied by XRD in the temperature interval from RT to  $T_{SS}$ . The following sequence of the phase transitions, contrary to the phase diagram, was observed for both alloys

$$\alpha(M/\beta) + \beta(\text{Zn}) - \alpha' + \beta(\text{Zn}) + \alpha(M/\alpha', \beta) - \alpha' + \beta(\text{Zn}) - \alpha_{SS}.$$

That result and the result of the present paper indicate that a change in the phase diagram is necessary in the region where the contents of Al and Zn are rather similar. Previous studies [7, 9, 10] show that the observed phase transitions in the alloys, in which the initial content of Zn is equal to or smaller than about 40 at%, are in a full agreement with the phase diagram [1, 6].

#### References

- [1] H. Löffler, *Structure and Structure Development in Al-Zn Alloys*, Akademie Verlag, Berlin (1995).
- [2] S. Popović, H. Löffler, B. Gržeta, G. Wendrock and P. Czurratis, *phys. stat. sol. (a)* **111** (1989) 417.
- [3] S. Popović, B. Gržeta, V. Ilakovac, R. Kroggel, G. Wendrock and H. Löffler, *phys. stat. sol. (a)* **130** (1992) 273.
- [4] S. Popović, B. Gržeta, H. Löffler and G. Wendrock, *Fizika A (Zagreb)* **4** (1995) 529.
- [5] S. Popović, B. Gržeta, H. Löffler, and G. Wendrock, *Lattice Constant of the Al-rich fcc  $\alpha$ -Phase in Contact with Various Kinds of Precipitates*, in Ref. [1], pp. 212-241.
- [6] H. Löffler, G. Wendrock and O. Simmich, *phys. stat. sol. (a)* **132** (1992) 339.
- [7] S. Popović, B. Gržeta, H. Löffler and G. Wendrock, *phys. stat. sol. (a)* **140** (1993) 341.
- [8] S. Popović, B. Gržeta, V. Ilakovac, H. Löffler and G. Wendrock, *phys. stat. sol. (a)* **141** (1994) 43.
- [9] S. Popović and B. Gržeta, *Croat. Chem. Acta* **72** (1999) 621.
- [10] S. Popović and B. Gržeta, *Mater. Sci. Forum* **321-324** (2000) 635.
- [11] S. Popović, B. Gržeta, B. Hanžek and S. Hajster, *Fizika A (Zagreb)* **8** (1999) 173.
- [12] S. Popović, *J. Appl. Cryst.* **4** (1971) 240; **6** (1973) 122.
- [13] S. Popović, *Cryst. Res. Technol.* **20** (1985) 552.

OVISNOST MIKROSTRUKTURE SLITINA Al-44 at% Zn I Al-48 at% Zn O  
TEMPERATURI

Primjenom rentgenske difrakcije in situ istraživali smo temperaturnu ovisnost mikrostrukture navedenih slitina. Slitine su bile prethodno podvrgnute različitim termičkim obradama: (i) brzom kaljenju s temperature čvrste otopine,  $T_{SS}$ , u vodi pri sobnoj temperaturi (uzorci WQ); (ii) sporom hlađenju od  $T_{SS}$  do sobne temperature i starenju pri sobnoj temperaturi (uzorci SC). Budući da su nakon starenja uzorci SC bili bliži ravnotežnom stanju nego uzorci WQ, mikrostruktura dviju skupina uzoraka ovisila je o temperaturi na različit način. Uzorci SC bili su prevedeni u stanje čvrste otopine,  $\alpha_{SS}$ , na temperaturi oko 720 K, a uzorci WQ na oko 880 K. Umjesto faznih pretvorbi koje bi se očekivale prema faznom dijagramu, opazili smo ovaj niz pretvorbi za obje slitine:  $\alpha(M/\beta)+\beta(Zn) - \alpha'+\beta(Zn)+\alpha(M/\alpha',\beta) - \alpha_{SS}$ . Slično ponašanje nađeno je i za slitine bogatije cinkom, Al-54 at% Zn i Al-62 at% Zn.